

Mathematical *form factor* studies on the effect of water on airborne particles morphology using a bi-dimensional TEM image processing

Rodolfo Cucchiella,^a Giuseppe Falini,^b Massimo Ferri,^a Milena Stracquadanio^c and Claudio Trombini^{*b}

Received 24th April 2008, Accepted 13th October 2008

First published as an Advance Article on the web 7th November 2008

DOI: 10.1039/b806940a

Mathematical morphology is a tool for extracting image components that are useful for representation and description. The technique consists of a set-theoretic method of image analysis providing a quantitative description of geometrical structures. A simple application of mathematical morphology to a bi-dimensional processing of TEM images of airborne particles allows us to distinguish between particles grown and/or transported in atmosphere under dry conditions or in rainy days by a simple comparison of the corresponding image form factors. The form factors range in the 0.385–0.031 interval in the case of particles sampled in rainy days, and in the 0.103–0.006 interval in the case of non-rainy conditions. The same classification criterion was applied to filters collected under dry conditions and plunged in water. The results demonstrate that a morphological change may be artificially induced to the particle structure. The artificially wet particles, indeed, display an apparent contraction of their structures evidenced by a two-fold increase of the average values of their form factors. The last experiment roughly simulates the impact of particles on membranes of the respiratory tract.

Introduction

Atmospheric fine and ultra-fine carbonaceous particles, often referred to as “diesel soot”, are of current interest because of two reasons. (i) They exert adverse effects on health,^{1,2} as witnessed by epidemiological and toxicological studies dealing with prenatal and early childhood health effects,³ asthma and other pediatric morbidities,⁴ respiratory health effects,⁵ adverse chronic cardiopulmonary effects,^{6,7} and carcinogenicity.⁸ (ii) Atmospheric fine and ultra-fine particles influence the climate by scattering or absorbing light and by acting as cloud nuclei.⁹ In particular, carbonaceous particles directly affect the earth's radiation balance by absorbing solar radiation, thus contributing to the atmospheric warming.¹⁰

A major contribution to the total budget of atmospheric particulate matter in urban and industrial areas, is given by gasoline and diesel powered engines exhausts, which deliver soot, mainly consisting of carbonaceous primary nanoparticles.^{11–13} Combustion-generated nanoparticles are composed of carbon spherules typically sized between 20 and 50 nm,^{14–16} and held together by non-directional cohesive forces (van der Waals interactions, electrostatic interactions, π -stacking interactions) to form branched aggregates and clusters of variable size that contain up to hundreds of individual spherules.^{15,17,18} Once emitted to the atmosphere, the condensation of primary particles

or the formation of new volatile particles through nucleation gives rise to secondary particles.

In addition to composition and size distribution, particle morphology is an important factor affecting their toxicity, optical properties,^{19,20} and lifetime in the atmosphere.²¹

After the first morphological studies on airborne particulate collected in urban areas using transmission electron microscopy (TEM),²² efforts have been focused on determining the effect on morphology of primary sources, fuels and combustion conditions. For instance, the engine load affects particles morphology and fractal dimensions of particles.²³ Particles from exhausts of a direct-injected heavy-duty diesel engine working under different operating conditions,^{20,24} as well as particles emitted from spark ignition engines of light-duty vehicles have been examined by TEM.²⁵ Moreover, morphological investigations by electron microscopy has been extended to particles deriving from combustion of various fuels such as residual oil,²⁵ or coal and tires in power plants.²⁶

Besides to its primary source, particle morphology depends on general weather conditions such as temperature and relative humidity.²⁷

The research question in this study was to verify if the structure of airborne particles is affected by water and to describe this effect in a quantitative way.

The experimental design involved collecting particles by sampling PM_{2.5} in quartz fiber filters (QFF), subjecting particles to an extensive TEM analysis, and processing TEM images with mathematical morphology (MM) techniques.

Mathematical morphology (MM) provides a powerful tool for TEM image processing. In this study MM gives us a solution to quantitatively distinguish between particles grown and transported under dry conditions and particles exposed to the action of liquid water during transport (rain) or by impact on an aqueous phase.

^aDipartimento di Matematica - Università di Bologna, Piazza di Porta S. Donato 5, 40126 Bologna, Italy

^bDipartimento di Chimica “G. Ciamician”, Università di Bologna, via Selmi 2, 40126 Bologna, Italy. E-mail: claudio.trombini@unibo.it; Fax: +39 051 2099456; Tel: +39 051 2099513

^cDipartimento di Chimica Industriale e dei Materiali, Università di Bologna, Viale del Risorgimento 4, 40136 Bologna, Italy

Image processing. Theoretical methodology

The theoretical tools for image processing in MM are three operations: thresholding, erosion and dilation.

A grey-tone image is a matrix M , whose entries are integer numbers in the interval $[0, 255]$, where 0 represents black, and 255 white. A binary image is a matrix N whose entries are either 0 (black) or 1 (white). *Thresholding* consists in deciding a *threshold value* L and substituting a grey-tone image M with a binary image N of the same size, where each $N(i,j) = 0$ if $M(i,j) < L$, and $N(i,j) = 1$ if $M(i,j) \geq L$.

Erosion and *dilation* are substitutions of a given binary image N with a new one. They both depend on the choice of a *structuring element*, i.e. an auxiliary matrix B (usually small with respect to N) whose indices may be null or negative. *Erosion* substitutes the matrix N with a matrix N' where $N'(i,j) = 1$ if and only if $N(i + h, j + k) = 1$ for all h, k such that $B(h, k) = 1$, and $N'(i,j) = 0$ otherwise. *Dilation* substitutes N with a matrix N'' where $N''(i,j) = 1$ if and only if there exists at least one h and one k such that $N(i + h, j + k) = 1$ and $B(h, k) = 1$, and $N''(i,j) = 0$ otherwise. *Erosion* and *dilation* are the basic manipulations in mathematical morphology.²⁸

On all images of this research, both of training and test sets, the threshold was set at two different values: $T1 = 193$ and $T2 = 200$, in order to catch different detail levels. The choice of $T1$ and $T2$ had been done by first applying four different thresholds to some randomly chosen images. The lowest and highest thresholds turned out to be unfit, since they destroyed the relevant information of some of the images. The two middle thresholds were then progressively tuned until they gave satisfactory results on all of them. We decided to keep two different (although close) values in order to test the form factor method, both with greater and rougher detail.

The morphological processing was then performed by applying three dilations in sequence, followed by three erosions. The structuring element was always a square of side three whose entries were all equal to 1.

As a parameter for assessing the compactness of the image, we choose the *form factor* (ff) expressed as:

$$ff = 4\pi A/p^2$$

where A is the area and p is the perimeter of the region of interest. This number equals 1 if and only if the region of interest is a full disc, and is gradually closer to 0 the more indented and disconnected it is.

In order to test the hypothesis that “wet” particles are more compact, we have computed the ff of all images after thresholding both with $T1$ and $T2$, and carrying out the sequence of dilations and erosions. The whole set of black pixels was then considered to be the region of interest of each image. Manual post-processing turned out to be necessary, for getting rid of the grid support from the images. Nothing could be done for correcting the images in which the region of interest is not totally contained in the frame. This is of course a drawback that affects the computation of the ff .

What we obtain is a two-class classifier. It is based on a cutoff value F of the ff . Explicitly, the program classifies an image as *positive* (i.e. “wet” particle) if $ff \geq F$, *negative* (i.e. “dry” particle)

otherwise. Of course, even without the aforementioned problems, one should always expect some “dry” particle images to have $ff \geq F$ (*false positive*) and some wet ones to have $ff < F$ (*false negative*). Two parameters are used for assessing the quality of a classifier: *sensitivity* (Se) and *specificity* (Sp). They are based on an *a priori* knowledge of the real status of the sample as dry or wet (*ground truth*) which will be considered as absolute.

Se is defined as the ratio

$$Se = (\# \text{ of wet samples classified as such}) / (\text{total } \# \text{ of wet samples})$$

and Sp as

$$Sp = (\# \text{ of dry samples classified as such}) / (\text{total } \# \text{ of dry samples})$$

where denominators refer to the ground truth.

So, a high sensitivity means that the classifier yields few false negatives, and a high Sp that there are few false positives.

Of course, it would be desirable to have both parameters equal to 1, but this is very rarely possible in practice. A very low cutoff F may yield a high Se , even equal to 1, but at the cost of a low Sp . By gradually raising F , we shall be able to increase Sp , but eventually Se will lessen. Actually, by using F as a parameter, we can trace a curve, called Receiver Operating Characteristic (*ROC curve*), traditionally plotted with $1 - Sp$ as the abscissa x and Se as the ordinate y , which depicts the global behavior of the classifier. The farther from the diagonal $y = x$ it is, the better the classifier.

Given the ROC curve of a classifier, it can be used in some different ways for choosing a “good” cutoff value F . In the ideal case of a perfect classifier, the ROC curve would simply follow the left and upper sides of the square $[0, 1] \times [0, 1]$ and the optimal cutoff, actually splitting the two classes, would correspond to the upper left corner. With a real ROC curve, one must be content with an approximation. At least two cutoff values are available: the value F' corresponding to the intersection of the ROC curve with the diagonal $y = 1 - x$, and the value F'' corresponding to the point of the ROC curve nearest to the upper left corner.

Particle sampling and TEM observations

Typical urban particles have been investigated. In particular, $PM_{2.5}$ was sampled in the Bologna city centre ($44^\circ 29' 47'' N$; $11^\circ 21' 14'' E$), in an area where particulate matter had been previously investigated.^{29,30} The Bologna neighborhood does not host heavy industries, thus urban traffic and residential combustion represent the prevailing sources of airborne particulate matter.

$PM_{2.5}$ samples were collected on quartz fiber filters (QFF) (QF 20 Schleicher & Schuell) by means of a Bravo PM HV TCR Tecora instrument equipped with a EN LVS $PM_{2.5}$ size selective inlet, which complies with the European norm EN 12341 (air flux = $2.3 \text{ m}^3 \text{ h}^{-1}$). Sampling details are given in ref. 30.

Henceforth, samples and particles collected in non-rainy days are operationally defined as “dry” samples or particles, those collected in rainy days are defined as “naturally wet”. No attempts were done to correlate particles to the mean relative humidity of the sampling day. To test whether impact with liquid water brings about morphological changes to particles, a few QFF's sampled in non-rainy conditions were cut in two portions.

A half filter was dipped either in milliQ® water or in a physiological solution for 12 hours in a Petri dish, then dried in a desiccator for 48 hours at room temperature ($T \sim 20\text{--}25\text{ }^{\circ}\text{C}$). These last samples were referred as “artificially wet”.

To collect particles on a suitable TEM support, two approaches were used: (i) ten 35 mm copper grids, leaned down on the QFF surface, captured impacting particles during sampling; (ii) particles were mechanically transferred from a QFF to grids by softly rubbing grids on the QFF surface. Grids were stored at room temperature in a TEM grid storage box until the analysis. The digitized TEM images were collected by means of a Philips CM100 TEM instrument at a voltage of 80 KV, using a high resolution closed-coupled device (CCD) camera. The TEM was operated in bright field mode. The images were divided in two sets. The first set consisted of 31 images of “dry” particles and 32 images of “wet” particles and constituted the *training set*. The second one consisted of 32 images randomly extracted from the entire pool of images from dry and wet samples. It constituted the *test set*. Of course, the images used in the test set were not present in the training set to avoid any bias effect.

All the TEM images confirmed that particles collected in this urban site mainly derive from combustion processes, since they consist of branched chains aggregations of elementary units having the shape of spherules with diameter ranging from 20 to 50 nm, as widely documented in the literature.^{14–18} In the samples examined, most of submicronic particles were carbonaceous particles. Fig. 1a shows the typical TEM image of branching ultrafine soot aggregate, which is formed from individual primary spherules of 20–50 nm size. Generally, carbon speciation of diesel exhaust and urban particulate matter differentiates between two principal fractions: elemental carbon (EC) and organic carbon (OC). EC normally has almost no hydrogen content and is usually considered to be a product of combustion of fossil fuels. OC has a higher hydrogen content and lower oxidation resistance. Morphology of OC particles is that of big spherical particles (above 50 nm) either isolated or attached to the soot aggregates. In Fig. 1b an OC-type carbonaceous particle attached to soot aggregate is indicated by the arrow.^{31,32} The TEM images collected from wet samples (Fig. 1c, d) do not

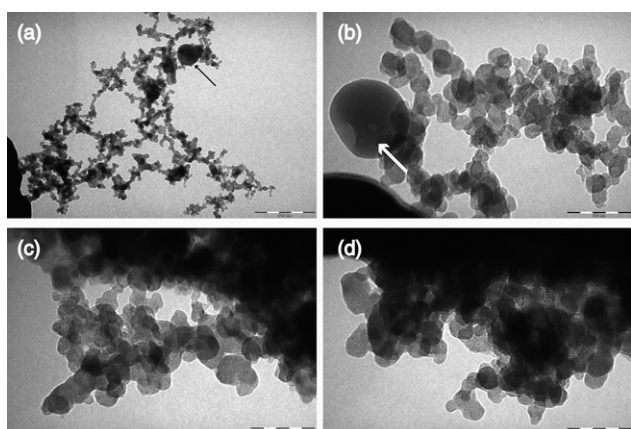


Fig. 1 Bright-field TEM images of particulate matter. (a) and (b) show two magnifications of “dry” particles; (c) “naturally wet” particles; (d) “artificially wet” particles. The OC-type carbonaceous particle attached to the soot aggregate is indicated by the arrow. Scale bars: (a) 500 nm; (b), (c) and (d) 100 nm.

show the presence of OC particles. Only spherules from 20 to 50 nm are observed, with the same size of the dry samples, but with a different shape, aggregation and branching.

Results and discussion

This study focused on the following objectives:

(i) to prove that airborne nano-structured particles show different morphology depending on they are sampled in rainy or non-rainy days; more compact structures are observed in rainy days with respect to those of particles sampled under dry conditions.

(ii) To propose a simple bi-dimensional image processing providing simple numerical descriptors for the ffs that adequately characterize and classify the nanostructured particles on the basis of a contact/non-contact with water.

(iii) To verify that dry particles after contact with water by plunging them into pure water or a pH 7 phosphate-buffered solution, undergo an appreciable and measurable morphological change, which consists, from a qualitative point of view, of a particle shrinking. The result is a substantial decrease of the empty volume between particle chains.

The experimental design was as follows. Two sets of images were provided; the ground truth (dry/wet) of the *training set* was explicit; for the *test set* it was hidden. All images of both sets were processed as described, with the two thresholds $T1 = 193$ and $T2 = 200$. For each of these thresholds the ROC curve was traced, and the cutoff values were derived: F' (the intersection of the ROC curve with the diagonal $y = 1 - x$) is denoted as $F1$ for $T1$ thresholding and $F3$ for $T2$; F'' (the point of the ROC curve nearest to the upper left corner) is denoted respectively as $F2$ and $F4$, as shown in Fig. 2.

Because of closeness of the two pairs of cutoff values, only one of the two points was chosen for our computations. Thus, the images of the test set have been classified by using $F2$ and $F4$ as cutoff values for the ff. Table 1 collects the ffs of the training set of images, while Table 2 shows ffs and classification for each image of the test set, against the ground truth; false negative and false positive are evidenced. The use of the lower threshold for binarization of images seems more efficient in keeping the relevant features sufficiently unaltered. However, with both thresholding values, there are three images which escape classification (Table 2, #18, #21 and #23).

Using this bi-dimensional image processing to determine the ff of airborne carbonaceous particles, a simple method to measure

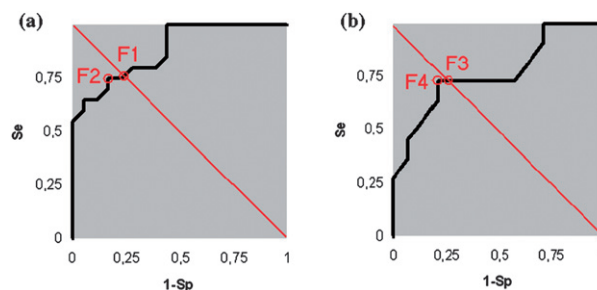


Fig. 2 ROC curves for $T1$ (a) and $T2$ (b) thresholding. Se and Sp indicate *sensitivity* and *specificity*, respectively.

Table 1 Form factors evaluated from the training set

	Dry set Form factor	Wet set	
		Form factor	Wetting mode ^a
1	0.0393	0.0700	nat.
2	0.0431	0.1809	nat.
3	0.0374	0.3395	nat.
4	0.0541	0.3848	nat.
5	0.0575	0.0498	nat.
6	0.0394	0.1949	nat.
7	0.0133	0.1419	nat.
8	0.0064	0.1962	nat.
9	0.0133	0.0689	nat.
10	0.0195	0.0581	nat.
11	0.0144	0.1266	nat.
12	0.0092	0.1667	nat.
13	0.0380	0.3113	nat.
14	0.0351	0.0602	nat.
15	0.0502	0.0308	nat.
16	0.1034	0.1429	nat.
17	0.0806	0.1113	nat.
18	0.0611	0.0366	nat.
19	0.0347	0.0228	nat.
20	0.0605	0.0294	nat.
21	0.0162	0.0765	nat.
22	0.0161	0.0319	nat.
23	0.0110	0.1041	nat.
24	0.0059	0.1211	nat.
25	0.0093	0.0525	nat.
26	0.0200	0.0734	art.
27	0.0336	0.0214	art.
28	0.0116	0.0306	art.
29	0.0174	0.0550	art.
30	0.0687	0.1074	art.
31	0.0310	0.0675	art.
32		0.0889	art.

^a Nat. indicates sample collected under “naturally wet” conditions; art. indicates “artificially wet” samples.

Table 2 Form factors and classification of test images; false negative and false positive are evidenced

	Form factor	Classification F2 = 0.058	Classification F3 = 0.051	Ground truth
1	0.2521	wet ^a	wet	wet
2	0.1591	wet	wet	wet
3	0.1504	wet	wet	wet
4	0.0515	dry ^b	wet	dry
5	0.0399	dry	dry	dry
6	0.0253	dry	dry	dry
7	0.0272	dry	dry	dry
8	0.0548	dry	wet	dry
9	0.0463	dry	dry	dry
10	0.0395	dry	dry	dry
11	0.0847	wet	wet	wet
12	0.0600	wet	wet	wet
13	0.0090	dry	dry	dry
14	0.0243	dry	dry	dry
15	0.0824	wet	wet	wet
16	0.0964	wet	wet	wet
17	0.2309	wet	wet	wet
18	0.0326	dry	dry	wet
19	0.0364	dry	dry	wet
20	0.1081	wet	wet	wet
21	0.0419	dry	dry	wet
22	0.0316	dry	dry	dry
23	0.0734	wet	wet	dry
24	0.0391	dry	dry	dry
25	0.0189	dry	dry	dry
26	0.0086	dry	dry	dry
27	0.0131	dry	dry	dry
28	0.0329	dry	dry	dry
29	0.0083	dry	dry	dry
30	0.2372	wet	wet	wet
31	0.1049	wet	wet	wet
32	0.1902	wet	wet	wet

^a Wet indicates sample collected in wet conditions. ^b Dry indicates samples collected in dry conditions.

the particle shrinking effect due to exposure to water is proposed. Indeed, the ff of “dry” particles varies around the average value of 0.032 with a standard deviation of 0.023, the highest value observed being 0.103 (Table 3). On the other hand, “wet” particles show an average ff of 0.121 with a standard deviation of 0.087 and a maximum value observed of 0.385.

Even though a partial overlap of the ff ranges exists (borderline images where an unambiguous assignment is not possible), values higher than 0.087 (the 90% of wet samples) clearly are associated to airborne particles grown and/or transported in rainy days, while particles possessing a ff < 0.03 are definitely “dry particles” (Fig. 3).

This simple application of MM to TEM images looks as a straightforward tool to classify a particle originated and/or transported under dry or rainy conditions.

Let’s now come to the last question, do morphology changes occur in dry particles after contact with liquid water?

The interaction of fine airborne particles with liquid water has a terrific interest when biological membranes are involved. Recently, light has been shed onto the interaction between lung lining liquid and inhaled ambient particles.³³ An aggregation process has been observed to occur in this aqueous micro-layer, and it was claimed to be driven by the proteins present in the lining liquid. The new greater and more dense particles are more

Table 3 Statistical data from form factors calculated from TEM images

	Average value	St. dev.	Max ^a	Min ^a
dry	0.032	0.023	0.103	0.003
wet	0.121	0.087	0.385	0.021
wet-nat.	0.137	0.092	0.385	0.023
wet-art.	0.063	0.027	0.107	0.021

^a max and min indicate the maximum and minimum value, respectively; **wet** indicates sample collected in wet conditions; **dry** indicates samples collected in dry conditions; **wet-nat.** indicates sample collected under “naturally wet” conditions; **wet-art.** indicates “artificially wet” samples.

easily phagocytized by macrophages. The neat result is a more efficient particle clearance in the lung lining fluid, thus rendering particle aggregation a kind of lung protective process.

To prove that water brings morphological changes to particles one half of few QFF’s sampled in non-rainy conditions has been dipped either in milliQ® water or in a physiological solution and then dried. Images taken from the untreated half QFF and the wetted half have been compared.

The study carried out in a set of 7 filters sampled in dry days revealed that the simple action of liquid water shrinks aggregates and this phenomenon can be measured by comparing the ff of particles collected from the original and water-treated portions

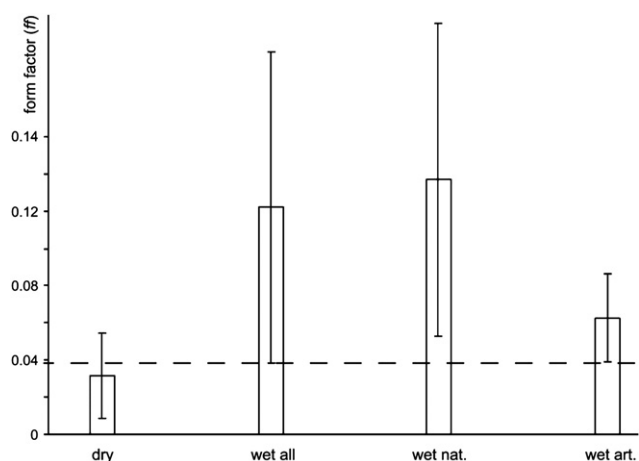


Fig. 3 Histogram showing the form factors (ff) calculated from “dry” and “wet” particles. The dashed line indicates the ff threshold below which the particle is classified as dry.

of the filters. While the average ff for the untreated particles is 0.032, the average value of particles ff from the water treated QFFs increases to 0.063, a clear indication that the direct contact with water is responsible for structure compression.

Conclusions

In conclusion, applying MM to a bi-dimensional processing of TEM images of airborne particles, we demonstrated the research hypothesis, that particles grown and/or transported in the atmosphere under dry conditions or in rainy days show a different morphology. The application of MM to TEM images proved to be an efficient tool to unambiguously confirm that in “wet” particles the branched aggregates and clusters of individual spherules of 20–50 nm are more compact with smaller inter-chain volumes with respect to “dry” particles. Beside to support the original hypothesis, MM provided a quantitative measure of the different morphology of the two kinds of particles, “wet” or “dry”, resulting in defined ffs ranges. The change in morphology may be also artificially induced on a “dry” particle by simply plunging it in water. The result is an apparent contraction of particle structure evidenced by a significant increase (two-fold increase of the average values) of the corresponding form factors. A similar contact with liquid water occurs when particles are inhaled and deposited on the respiratory tract membranes (nose, pharynx, gas exchange airways, etc.). Our results support a recent observation of an enhanced aggregation of particles impacting on the lung lining liquid, exploiting scanning electron microscopy (SEM), atomic force microscopy, and X-ray photon spectroscopy.³³

References

- 1 N. Englert, Fine particles and human health - a review of epidemiological studies, *Toxicol. Lett.*, 2004, **149**, 235–242.
- 2 D. W. Dockery and C. A. Pope, Acute respiratory effects of particulate air pollution, *Annu. Rev. Public Health*, 1994, **15**, 107–132.
- 3 M. Lacasana, A. Esplugues and F. Ballester, Exposure to ambient air pollution and prenatal and early childhood health effects, *Eur. J. Epidemiol.*, 2005, **20**, 183–199.

- 4 L. Trasande and G. D. Thurston, The role of air pollution in asthma and other pediatric morbidities, *J. Allergy Clin. Immunol.*, 2005, **115**, 689–699.
- 5 K. Donaldson, L. A. Jimenez, I. Rahman, S. P. Faux, W. MacNee, P. S. Gilmour, P. J. A. Borm, R. P. F. Schins, T. Shi and V. Stone, Respiratory health effects of ambient air pollution particles: Role of reactive species, *Lung Biology in Health and Disease*, 187 (*Oxygen/Nitrogen Radicals*), 2004, 257–288.
- 6 M. Lippmann, T. Gordon and L. C. Chen, Effects of subchronic exposures to concentrated ambient particles in mice: IX. Integral assessment and human health implications of subchronic exposures of mice to CAPs, *Inhal. Toxicol.*, 2005, **17**, 255–261.
- 7 J. Heinrich and H. E. Wichmann, Traffic related pollutants in Europe and their effect on allergic disease, *Curr. Opinion Allergy Clin. Immunol.*, 2004, **4**, 341–348.
- 8 R. M. Harrison, D. J. T. Smith and A. J. Kibble, What is responsible for the carcinogenicity of PM_{2.5}?, *Occupat. Environ. Med.*, 2004, **61**, 799–805.
- 9 J. H. Seinfeld and S. N. Pandis, *Atmospheric Chemistry and Physics. From Air Pollution to Climate Change*, John Wiley and Sons, New York, 1998.
- 10 H. Burtscher, Measurement and characteristics of combustion aerosols with special consideration of photoelectric charging and charging by flame ions, *J. Aerosol Sci.*, 1992, **23**, 549–595.
- 11 T. J. A. Alander, A. P. Leskinen, T. M. Raunemaa and L. Rantanen, Characterization of diesel particles: effects of fuel reformulation, exhaust after treatment, and engine operation on particle carbon composition and volatility, *Environ. Sci. Technol.*, 2004, **38**, 2707–2714.
- 12 T. Huai, S. D. Shah, M. J. Wayne, T. Younglove, D. J. Chernich and A. Ayala, Analysis of heavy-duty diesel truck activity and emissions data, *Atm. Environ.*, 2006, **40**, 2333–2344.
- 13 H. Song, N. Ladommatos and H. Zhao, Morphology, size distribution, and oxidation of diesel soot, *J. Energy Inst.*, 2004, **77**, 26–36.
- 14 IPCC. Synthesis report. 2001; available at: www.grida.no/climate/ipcc_tar/vol4/english/index.htm.
- 15 H. X. Chen and R. A. Dobbins, Crystallogenes of particles formed in hydrocarbon combustion, *Combust. Sci. Technol.*, 2000, **159**, 109–128.
- 16 L. H. van Poppel, H. Friedrich, J. Spinsby, S. H. Chung, J. H. Seinfeld and P. R. Buseck, Electron tomography of nanoparticle clusters and implications for atmospheric lifetimes and radiative forcing of soot, *Geophys. Res. Lett.*, 2005, **32**, L24811.
- 17 J. Lahaye and F. Ehrburger-Dolle, Mechanisms of carbon black formation: correlation with the morphology of aggregates, *Carbon*, 1994, **32**, 1319–1324.
- 18 L. E. Murr and J. J. Bang, Electron microscopy comparisons of fine and ultra-fine carbonaceous and non-carbonaceous airborne particulates, *Atm. Environ.*, 2003, **37**, 4795–4806.
- 19 E. F. Mikhailov, S. S. Vlasenko, I. A. Podgorny, V. Ramanathan and C. E. Corrigan, Optical properties of soot-water drop agglomerates: an experimental study, *J. Geophys. Res. [Atmospheres]*, 2006, **111**(D7), D07209/1–D07209/16.
- 20 U. Mathis, M. Mohr, R. Kaegi, A. Bertola and K. Boulouchos, Influence of Diesel Engine Combustion Parameters on Primary Soot Particle Diameter, *Environ. Sci. Technol.*, 2005, **39**, 1887–1892.
- 21 A. K. K. Virtanen, J. M. Ristimaeki, K. M. Vaaraslahti and J. Keskinen, Effect of Engine Load on Diesel Soot Particles, *Environ. Sci. Technol.*, 2004, **38**, 2551–2556.
- 22 L. Paoletti, B. De Berardis and M. Diociaiuti, Physico-chemical characterization of the inhalable particulate matter (PM₁₀) in an urban area: an analysis of the seasonal trend, *Sci. Total Environ.*, 2002, **292**, 265–275, and references therein.
- 23 R. K. Chakrabarty, H. Moosmüller, W. P. Arnott, M. A. Garro and J. Walker, Structural and Fractal Properties of Particles Emitted from Spark Ignition Engines, *Environ. Sci. Technol.*, 2006, **40**, 6647–6654.
- 24 A. Neer and U. O. Koylu, Effect of operating conditions on the size, morphology, and concentration of submicrometer particulates emitted from a diesel engine, *Comb. and Flame*, 2006, **146**, 142–154.
- 25 Y. Chen, N. Shah, F. E. Huggins and G. P. Huffman, Investigation of the microcharacteristics of PM_{2.5} in residual oil fly ash by analytical

-
- transmission electron microscopy, *Environ. Sci. Technol.*, 2006, **40**, 6553–6560.
- 26 R. Gieré, M. Blackford and K. Smith, TEM Study of PM_{2.5} Emitted from Coal and Tire Combustion in a Thermal Power Station, *Environ. Sci. Technol.*, 2006, **40**, 6235–6240.
- 27 D. Ferry, J. Suzanne, S. Nitsche, O. B. Popovitcheva and N. K. Shonija, Water adsorption and dynamics on kerosene soot under atmospheric conditions, *J. Geophys. Res. [Atmospheres]*, 2002, **107**(D23), AAC22/1–AAC22/10.
- 28 J. Serra, *Image analysis and mathematical morphology*, Academic Press, London, 1982.
- 29 M. Stracquadanio, G. Apollo and C. Trombini, A Study of PM_{2.5} and PM_{2.5}-associated polycyclic aromatic hydrocarbons at an urban site in the Po Valley (Bologna, Italy), *Water Air Soil Pollution*, 2007, **179**, 227–237.
- 30 M. Stracquadanio, D. Bergamini, E. Massaroli and C. Trombini, Field evaluation of a passive sampler of polycyclic aromatic hydrocarbons (PAHs) in an urban atmosphere (Bologna, Italy), *J. Environ. Monit.*, 2005, **7**, 910–915.
- 31 Y. Chen, N. Shah, F. E. Huggins and G. P. Huffman, Microanalysis of ambient particles from Lexington, KY, by electron microscopy, *Atm. Environ.*, 2006, **40**, 651–663.
- 32 M. Schnaiter, M. Gimmler, I. Llamas, C. Linke, C. Jäger and H. Mutschke, Strong spectral dependence of light absorption by organic carbon particles formed by propane combustion, *Atmos. Chem. Phys. Discuss.*, 2006, **6**, 1841–1866.
- 33 M. Kendall, T. D. Tetley, E. Wigzell, B. Hutton, M. Nieuwenhuijsen and P. Luckham, Lung lining liquid modifies PM_{2.5} in favor of particle aggregation: a protective mechanism, *Am. J. Physiol. Lung Cell. Mol. Physiol.*, 2002, **282**, L109–L114.